

Imaging and Mesh Generation Issues in Patient-specific Simulation Studies of Coronary Hemodynamics

Mayr M.¹ and B. Quatember¹

¹Division of Diagnostic Radiology II, Innsbruck Medical University, Innsbruck, Austria
E-Mail: Bernhard.Quatember@uibk.ac.at

Keywords: *Image-based simulation, modelling, mesh generation, medical imaging, segmentation*

EXTENDED ABSTRACT

In our simulation studies of coronary hemodynamics, which are described in the companion paper entitled “Image-based Simulation of the three-dimensional Coronary Blood Flow” (Quatember *et al.* 2007), imaging and mesh generation issues are emphasized, particularly the segmentation of the coronary arteries in biplane angiograms, the three-dimensional reconstruction of the coronary artery tree and the determination of the size of the elements in the CFD finite element mesh, which is used for numerical simulations of the patient’s blood flow. Despite the availability of powerful software tools, the largely automatic segmentation of the coronary arteries in biplane angiograms continues to be an extremely difficult task because of noise, artefacts and other flaws which deteriorate the image quality. Since classical methods would not be able to provide satisfactory results, we developed an advanced segmentation technique based on the fact that the coronary arteries have a tree-like tubular structure. Our approach utilises a differential-geometric criterion. In particular, we developed a skeleton-based technique for the representation of the centre lines of the coronary arteries as well as special border detection procedures. Our three-dimensional reconstruction method yields a representation of the geometry of the coronary artery tree in the form of a wire frame model. We will also deal with the problems arising from the need for the generation of a high-quality mesh that is required for our numerical simulations of the coronary hemodynamics with the finite element method. Our imaging and mesh generation procedures are computationally expensive. The computations will be carried out in parallel within the framework of the newly-established “Austrian GRID.”

1 INTRODUCTION

In order to develop a computer system for the simulation of coronary hemodynamics, a precise knowledge of the geometry of the coronary (epicardial) arteries of the patient is required. The companion paper entitled

”Image-based Simulation of the three-dimensional Coronary Blood Flow“ (Quatember *et al.* 2007) deals with three-dimensional simulation studies of the blood flow, especially in stenosed sections of the coronary arteries. These are carried out numerically with the finite element method. In this paper, we focus on the determination of the patient’s coronary arteries and the generation of the mesh which is needed for the numerical simulation studies. An adequate knowledge of the geometry of the coronary arteries can only be acquired by means of medical imagery. Of all the imaging modalities that are currently being used in cardiology, biplane angiography yields the most accurate information. However, complicated image processing methods must be applied to separate the tree-like structure of the epicardial arteries from the rest of the image, especially from background structures. This separation is called segmentation. In this paper we will describe here the development of an advanced method for the largely automatic handling of this task that is based on differential-geometric criteria and the use of special border line detection algorithms. With our advanced method, we are not only able to distinguish the tubular structures of the coronary artery tree from the rest of the image, but can also suppress noise and background structures. Moreover, the method is able to eliminate the errors due to geometric unsharpness (blur) caused by the finite focal size of the X-ray tube. The segmented angiograms provide the basis for our three-dimensional reconstruction of the coronary artery tree and its representation in the form of a wire frame model. However, we will only describe this reconstruction process and the above-mentioned mesh generation in a very brief manner.

2 SEGMENTATION METHODS

A prerequisite for our patient-specific simulation approaches as described in the companion paper (Quatember *et al.* 2007) is a fairly precise knowledge of the geometry of the coronary (especially epicardial) arteries. As mentioned above, it is best to derive the geometry of the patient's coronary (epicardial) arteries from biplane angiograms. Complicated image processing methods are needed for the segmentation of the coronary artery tree, in other words for the separation of the tree-like structure of the coronary (epicardial) arteries from the rest of the image, especially from background structures. We will describe our method for a largely automatic segmentation and briefly deal with its implementation in a GRID environment (Austrian GRID).

2.1 Overview of our segmentation approach

Biplane angiograms are taken with biplane angiography systems that consists of two "X-ray tube - image intensifier" pairs. The X-ray tubes cast shadows of the coronary arteries, when filled with a contrast medium, onto image intensifiers. The resulting two images, the biplane angiograms, are thus central projections of the flow domain within the epicardial arteries. Figure 1 shows one such projection (Projection A). However, the finite focal size of the X-ray tube causes considerable geometric blurring, which leads to deterioration of the image quality. Despite the availability of advanced image processing software, performing this kind of segmentation continues to be an extremely difficult and challenging task. After it became clear that the straightforward application of classical image processing methods would fail, we developed an advanced segmentation technique based on the fact that the coronary (epicardial) arteries have a tree-like tubular structure with sections of different sizes. We exploit this *a priori* knowledge to separate the representation of the coronary artery tree (X-ray shadow of the contrast-medium-filled arteries) from noise, background structures, artefacts and other weak spots of the angiograms, thereby making use of Hessian filters and applying skeletonizing procedures. Moreover, we utilize a special software module to detect the border lines of the coronary artery tree, which also permits a correction of geometric blurring effects. Hence, our segmentation procedures can be divided into the following phases

- The Hessian artery enhancement filtering phase,
- The skeletonizing phase, and
- The border-line detection phase.

These will be described in detail below.

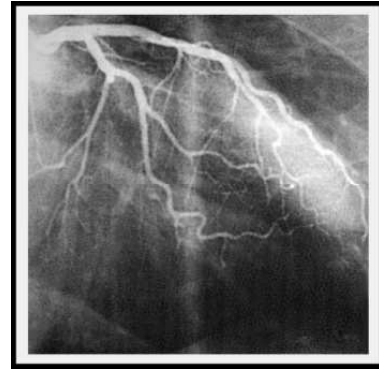


Figure 1. One Projection of a Biplane Angiography System

2.2 Hessian artery enhancement filtering phase

Our approach is based on a differential-geometric criterion (Mayr and Quatember 2005; Shriver and Slump 2002). It relies on the values of a so-called vesselness function which is derived from the eigenvalues λ_1 and λ_2 of the Hessian matrix H of the grey scale function belonging to the angiogram. These eigenvalues are functions of the grid point \vec{x} of the image; in the region of tubular structures, the following relationship holds:

$$|\lambda_1(\vec{x})| \gg |\lambda_2(\vec{x})| \quad (1)$$

The vesselness function (Shriver and Slump 2002) is defined as follows:

$$V(\vec{x}) = \begin{cases} 0 & \lambda_1(\vec{x}) < 0 \\ \exp\left(-\frac{R_B(\vec{x})^2}{2\beta_1^2}\right)[1 - \exp\left(-\frac{S(\vec{x})^2}{2\beta_2^2}\right)] & \text{otherwise} \end{cases} \quad (2)$$

in which

$$R_B(\vec{x}) = \frac{|\lambda_2(\vec{x})|}{|\lambda_1(\vec{x})|} \quad (3)$$

and

$$S(\vec{x}) = \sqrt{\lambda_1(\vec{x})^2 + \lambda_2(\vec{x})^2} \quad (4)$$

The scaling factors $\beta_1 > 0$ and $\beta_2 > 0$ influence the sensitivity to $R_B(\vec{x})$ and $S(\vec{x})$, respectively.

The value $V(\vec{x})$ is restricted to the interval $[0,1]$; positions in which the value 0 occurs in the image do not in any way resemble parts of a tubular structure, whereas a value close to 1 indicates a significant similarity to the structure of a vessel.

Our Hessian-based vessel enhancement filter is based on a multi-scale filtering approach. It can be used for all epicardial arteries regardless of their size. This filtering approach comprises the repeated execution of:

- A Gaussian smoothing followed by
- The calculation of a vesselness function by using the eigenvalues of the Hessian matrix of the grey scale function and

- The representation of the vesselness function as a grey scale image.

In calculating the iterations comprising the above three steps we vary the standard deviation (σ) of the Gaussian filter within an appropriately chosen range. As a result, we obtain a family of filtered images. Figure 2 shows the individual filtered images of this family, each representing the vesselness function for particular values of σ . This family of images is the basis for the subsequent skeletonizing phase.

2.3 Skeletonizing phase

From the family of filtered images described in the preceding paragraph we extract a new grey scale image by computing the maximum intensity projection (cf. Figure 3). It displays the crude structure of the coronary artery tree. By thresholding we generate a binary mask and then apply a thinning filter. In doing so, we obtain a skeletonized angiogram which can be seen in Figure 4.

2.4 Detection of border-line phase

The third phase of our segmentation process comprises the application of algorithms to detect the border lines (edges) of the representation of the coronary arteries in our angiograms (Hoffmann *et al.* 2002; Janssen *et al.* 2005). The border-line detection is a complicated procedure and constitutes the computationally most expensive stage of the segmentation process.

First, we carry out a smooth approximation to the discrete set of points (pixels) of the aforementioned skeleton image by calculating splines (approximating splines). These are regarded as preliminary centre lines of the coronary arteries. The tree-like structure of these splines is superimposed onto the original image (angiogram). At relatively short intervals we draw normals to these splines which we call scan lines. Along each member of this family of normals we acquire an intensity profile and then we analyse each of them thoroughly. In doing so, we confine

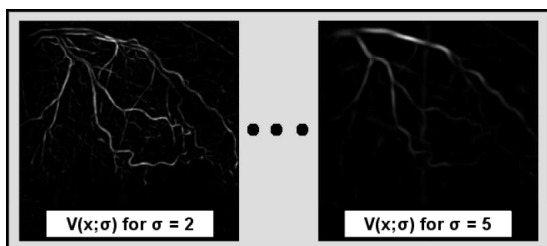


Figure 2. Multi-scale filtering approach: images after processing with a Hessian filter and varying values of sigma

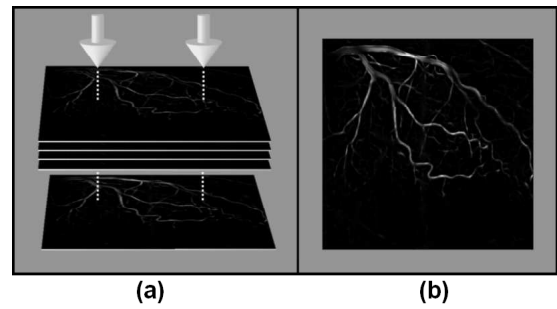


Figure 3. Maximum intensity projection: (a) approach; (b) resulting image

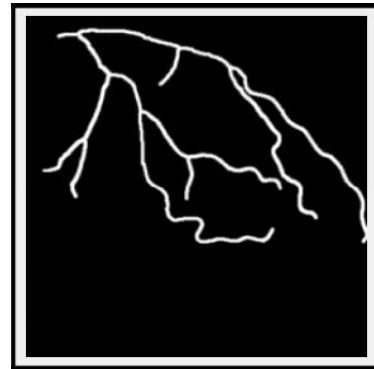


Figure 4. Skeleton of the coronary arteries

ourselves to an interval that is only marginally larger than the maximally expected size of the coronary (epicardial) artery. Primarily because of the finite focal spot size (apparent focal spot size) of the X-ray tubes, the relatively small coronary arteries will be considerably distorted by blurring. For a sophisticated analysis of these intensity profiles and especially to perform deblurring of the angiograms we have developed model-based border-line detection algorithms and, moreover, devised specific software components to suppress noise and background structures.

Our algorithms and software components differ distinctly from the known methods for analysing intensity profiles along scan lines and do not exhibit several of the limitations inherent in other known approaches. Our algorithms will be described in detail below, but first we want to provide a brief review of other approaches to border line detection.

Approaches to border line detection that are currently in use: In the literature, the following techniques have been described:

- Derivative-based techniques
- Densitometry-based techniques
- Model-based techniques

In derivative-based techniques, as described in the literature (Reiber *et al.* 1993), the first and second

derivatives of the intensity profiles in an appropriately chosen vicinity of the (preliminary) centre lines are calculated. The positions of the absolute extrema of either the first or the second derivative are the kind of points which are characteristic for the borders of the artery. More advanced techniques (Reiber *et al.* 1993) are based on a weighted average of both of these absolute extrema. However, the derivative-based methods, even the aforementioned advanced ones, are not sufficiently accurate and have proven to be completely inappropriate for the border-line detection of small arterial branches.

In the densitometry-based techniques (Silver *et al.* 1987), the integral of the intensity along the scan line is calculated (blurred image). The value of this integral is then compared with the simulation results of the integrals of the attenuated intensities behind contrast-medium-filled vessels (phantoms). Thereby it is assumed that the central projection is ideal (no blurring) and that the (assumed) luminal cross-sectional areas are known. The main disadvantage of this approach is the impossibility of dealing with cross-sectional areas that considerably deviate from circular or elliptical forms.

In current model-based approaches (Chan *et al.* 2000; Hoffmann *et al.* 2002), circular luminal cross-sectional areas are usually assumed. First, intensity profiles are calculated (simulated) for diameters ranging from 0.1 to 10 mm in increments of 0.1 mm, whereby the assumption is made that the central projection is ideal. These simulated intensity profiles are then convolved with the line-spread function of the X-ray tube so that the lack of sharpness (geometric blur and blurring effect of the image intensifier) is taken into consideration. The particular value for the diameter of the artery is chosen in such a way that the sums of the absolute differences between the intensity values of the pixels in the original image and the corresponding simulated intensity values of individual diameters yield a minimum. However, the approaches of this kind that are currently in use are not applicable to luminal cross-sectional areas with irregular shapes.

Development of an advanced border line detection method: Since the current methods do not fulfil all the requirements for an accurate border line detection, we developed an advanced technique. As mentioned earlier, the main difficulty in detecting the border lines of the coronary (epicardial) arteries in biplane angiograms is caused by the geometric blur due to the finite focal spot size of the X-ray tubes. This is particularly true for small arterial branches (diameter below 1.5 mm), since typical focal spot sizes (apparent focal spot sizes) are in the range of about 0.4 to 0.8 mm.

When we were developing the advanced border-line

detection method, we first thoroughly investigated the extent of the geometric blur. In doing so, we computed (simulated) the intensity profiles obtained with a contrast-medium-filled coronary artery both:

- In the ideal case of a central projection and
- In the real case of a finite focal spot size.

In doing so, we made the following simplifying assumptions to facilitate the computations:

- Parallel beam X-ray projection geometry
- Circular luminal cross-sectional area of the artery
- The direction of the longitudinal axis of the artery is orthogonal to the transversal plane through the central ray of the X-ray beam
- Errors caused by scattering effects are neglected
- Uniform focal spot intensity distribution are assumed.

The intensity profile (calibrated, overall magnification=1) can be calculated by using the attenuation equation

$$I(x) = I_0 e^{-\mu d(x)} \quad (5)$$

where x is a position along the horizontal axis; $I(x)$ is the function representing the intensity profile; I is the intensity of the incident X-ray beam; μ is the (linear) attenuation coefficient; and $d(x)$ is the distance between the incidence of the X-ray beam on and the exit from the contrast-medium-filled artery traversed by the X-ray beam at a particular position x .

Calculation (simulation) of the intensity profile in the ideal case of a central projection

Under our assumptions, the intensity profile of an artery with a circular luminal cross-sectional area with radius R can be mathematically described by Equation 5 where

$$d(x) = \sqrt{R^2 - x^2} \quad (6)$$

We thus obtain as the intensity profile in case of the ideal central projection $I_{cpi}(x)$

$$I_{cpi}(x) = I_0 e^{-2\mu\sqrt{R^2-x^2}} \quad (7)$$

For a thorough analysis of the intensity profiles $I_{cpi}(x)$ it is necessary to incorporate an analysis of their first and second derivatives $I'_{cpi}(x)$ and $I''_{cpi}(x)$.

The first derivative of the intensity profile (attenuated intensity) $I'_{cpi}(x)$ is calculated as follows:

$$I'_{cpi}(x) = I_0 \frac{2\mu x}{R^2 - x^2} e^{-2\mu\sqrt{R^2-x^2}} \quad (8)$$

For the second derivative of the intensity profile $I''_{cpi}(x)$, we obtain

$$I''_{cpi}(x) = I_0 \frac{2\mu}{R^2 - x^2} \left[\frac{R^2}{\sqrt{R^2 - x^2}} + 2\mu x^2 \right] e^{-2\mu\sqrt{R^2 - x^2}} \quad (9)$$

Calculation (simulation) of the intensity profile when the focal spot size is finite (0.5 mm)

We assume:

- An apparent focal size $a=0.5$ mm in the transversal direction of and, as previously mentioned,
- A uniform intensity distribution along the focal spot of the X-ray tube in the transversal direction.

We thus use the following line-spread function $L(x)$:

$$L(x) = \begin{cases} 0 & \text{for } x < 0, \\ \frac{1}{a} & \text{for } 0 \leq x \leq a, \\ 0 & \text{for } x > a \end{cases} \quad (10)$$

$L(x)$ has the property that

$$\int_{-\infty}^{\infty} L(x) dx = 1 \quad (11)$$

The intensity profile in case of the final focal spot size of $a=0.5$ mm $I_{ffs}(x)$ is calculated by carrying out the convolution of $I_{cpi}(x)$ with the line-spread function $L(x)$ as follows:

$$I_{ffs}(x) = \int_{-R-a}^{R+a} L(x-x') I_{cpi}(x) dx' \quad (12)$$

The above calculations of the function $I_{ffs}(x)$ and their derivatives $I'_{ffs}(x)$ and $I''_{ffs}(x)$ are carried out numerically.

In this case the simulated intensity profile $I_{ffs}(x)$ in case of a finite apparent focal spot size is quite different from the previously calculated $I_{cpi}(x)$ (see Equations 7); especially for small arterial luminal diameters (below 1.5 mm), the intensity profiles $I_{ffs}(x)$ and $I_{cpi}(x)$ differ considerably.

Fundamentals of the newly developed method for border line detection

For the application of our newly developed method it is necessary to know the apparent focal spot size and the line-spread function. The procedure utilises the simulation results for a finite focal spot size as described above.

In the following, we will confine ourselves to circular luminal cross-sectional areas, but in the future we will extend our considerations to luminal cross-sectional areas of other shapes. The character of the acquired intensity profiles along scan lines differs from the simulated intensity profiles due to noise and background structures. The noise can, however, be largely removed by using a smoothing filter. In our attempts to remove background structures (such as ribs and the diaphragm) we make use of the fact, that the dimensions of these structures exceed by far those of the coronary (epicardial) arteries. In particular, we lengthen the scan lines considerably and acquire the intensity profile along each elongated scan line. However, we exclude from consideration the intensity values within the aforementioned interval that is marginally larger than the maximally expected size of the artery from consideration. Instead we carry out a linear interpolation between the intensity values at the endpoints of this interval. We call an intensity profile obtained in such a way a background intensity profile. Along the elongated scan line we subtract the background intensity profile from the acquired intensity profile and thereby obtain what we call the undisturbed intensity profile $I_{ffs,undist,circ}(x)$.

Case 1: Border-line detection in an angiogram representing a coronary artery with a circular luminal cross-sectional area (orthogonal to the transversal plane through the central ray).

In the case of an angiogram representing a circular luminal cross-sectional area (orthogonal to the transversal plane through the central ray), the undisturbed intensity profile $I_{ffs,undist,circ}(x)$ will not significantly differ from the character of the simulated intensity profile $I_{ffs}(x)$, and we will thus be able to determine the border lines of the coronary artery in the following manner, which is quite straightforward:

At first, we calculate the intensity profiles $I_{ffs}(x)$ and their second derivatives $I''_{ffs}(x)$, and generate a look-up table for the function

$$d = g(m_1^{simul,circ,d} - m_2^{simul,circ,d}) \quad (13)$$

where $m_1^{simul,circ,d}$ and $m_2^{simul,circ,d}$ are the positions on the X-axis of those relative minima of $I''_{ffs}(x)$ which are situated in the neighbourhoods of both "knees" of the intensity profile $I_{ffs}(x)$.

By using this look-up table we are able to determine the borders as follows:

1. We acquire the undisturbed intensity profile $I_{ffs,undist,circ}(x)$ and its second derivative $I''_{ffs,undist,circ}(x)$.
2. On the X-axis we determine the positions of the minima of the second derivative of the profiles

in the neighbourhoods of both "knees" of the undisturbed intensity profile. We call these positions $m_1^{undist,circ}$ and $m_2^{undist,circ}$.

3. We then calculate the diameter d and the corresponding point of the final centre line P_{centre} (with the coordinate x_{centre}) that belongs to our particular cross-sectional area as follows:

$$d = g(m_1^{undist,circ} - m_2^{undist,circ}) \quad (14)$$

$$x_{centre} = \frac{m_1^{undist,circ} + m_2^{undist,circ}}{2} \quad (15)$$

4. We determine the points at the border as intersection points of this circle (with centre point P_{centre} and diameter d) with the x-axis.

Case 2: Border-line detection in an angiogram representing a coronary artery with a luminal cross-sectional area that deviates considerably from a circular shape (orthogonal to the transversal plane through the central ray).

In clinical practice, we have to reckon with luminal cross-sectional areas of coronary arteries that deviate considerably from a circular shape. Stenosed sections of the coronary arteries occasionally have a crescent-like cross section, and in diffuse coronary artery disease the cross sections are frequently irregular.

Our above-described border-line detection method has proven to be insensitive to changes in the shape of the cross section. Hence, we can use the above-described approach for arbitrary cross-sectional areas without severe restrictions.

3 3D RECONSTRUCTION

We developed a special method for the three-dimensional reconstruction which comprises the following steps:

- Automatic construction of the centre line in three-dimensional space. We define a space curve (spline curve) that passes through the points of intersection of the back projection rays belonging to the individual pairs of corresponding points (epipolar constraints).
- Automatic construction of normal planes at each of these points of intersection located on the space curve (c.f. Figure 5(b)).
- We draw back-projection rays from selected points of the border lines in both projections. The back-projection rays in the vicinity of a pair of corresponding points are intersected with the

normal plane that passes through the point of intersection belonging to this pair (c.f. Figure 5(a) and Figure 5(c)). We define four curves that pass through the aforementioned points of intersection on a normal plane. Subsequently, we construct an ellipse that approximates the aforementioned four curves. It is regarded as belonging to the inner surface of the coronary artery under consideration. In this way, we obtain a basic wire frame model of the arterial section.

For further details, please refer to Quatember and Mühlthaler (2003).

4 IMAGE-BASED GENERATION OF A HIGH-QUALITY MESH

In the following, only a brief overview of our image-based mesh generation procedures for stenosed sections of the epicardial arteries will be given. We decided to use a structured mesh with hexahedra as elements and to employ a multi-block approach. In order to obtain a high-quality mesh, we must adapt the size of the elements to the flow conditions. Since a consequent adaptive procedure with an *a posteriori* error analysis would consume too much time, we decided to employ specific *a priori* criteria for the adaptation. Although our criteria are in principle heuristic in nature, they nevertheless reflect a fair quantitative *a priori* knowledge relevant to the coronary artery under investigation. This quantitative knowledge is derived from *a posteriori* analyses of computed flow conditions in so-called reference flow domains. We have to bear in mind that in the entire field of CFD, heuristic *a priori* criteria are frequently taken as the basis for the generation of the mesh. In most cases, such criteria only reflect engineering experience and are thus not very reliable. From the outset of our development, we aimed at obtaining better *a priori* criteria for the mesh adaptation by using quantitative *a priori* knowledge.

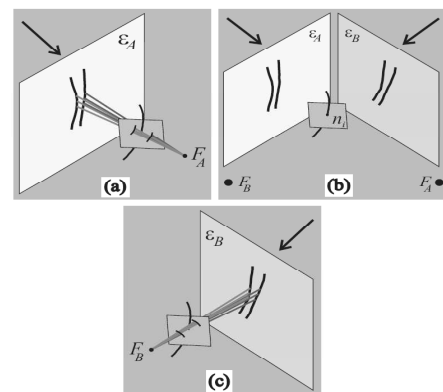


Figure 5. three-dimensional reconstruction; intersection of back projection rays with a normal plane.

At this stage of development, we confined ourselves to the mesh generation for concentric stenoses and eccentric stenoses with a relatively low degree of eccentricity. We defined a series of reference flow domains that are axially symmetric by systematically varying the luminal diameter and the geometry of the stenoses. In each reference domain, we generated an extraordinarily fine mesh and computed the flow conditions using the finite element method. With the results we devised a look-up table. The construction of a high-quality mesh depends not only on the geometry of the flow domain but also on the particular flow conditions (boundary conditions). Consequently we assumed as a boundary condition a volume flow through the section of the artery which is 50% above the typical rate of flow under resting conditions, the highest rate of flow that cardiologists will consider. Because we used an extraordinarily fine mesh, we could justifiably assume that the computed solution is the exact solution for the particular reference domain. We performed an *a posteriori* analysis that is based on this (virtually) exact solution. Specifically, we used a local error estimate for approximate solutions obtained with meshes comprising elements of a varying size. In doing so, we restricted ourselves to the interpolation error and explicitly neglected all other sources of error. In our *a posteriori* analysis, our goal was to determine the characteristics of an optimal mesh for the particular reference domain. However, real flow domains are not axially symmetric, even in the case of stenoses which cardiologists classify as being concentric. Hence, we must generate our meshes in genuine three-dimensional flow domains. In our heuristic approach, however, we exploit the above results for the (axially symmetric) reference flow domains as *a priori* criteria for the mesh construction as follows: From the aforementioned lookup table, we select the data for those two reference flow domains that come closest to the previously calculated parameters of the stenosed section of the coronary artery under investigation, and from those two reference flow domains, we choose the one whose data yield a finer mesh. We then employ the data from the chosen reference flow domain as control data for the generation of the mesh in the flow domain within the stenosed section under investigation. For further details, please refer to Quatember and Mühlthaler (2003).

5 CONCLUSIONS

In this paper we have described the development of an advanced segmentation method for biplane angiograms and have given an overview of the three-dimensional reconstruction of the coronary artery tree and the generation of a high-quality mesh within its flow domain. In the future, we will refine these methods and eliminate the restrictions and simplifications inherent in the present concept.

6 ACKNOWLEDGEMENT

The work described in this paper is partially supported by the "Austrian GRID" project, funded by the Austrian BMWF (Federal Ministry for Science and Research) under contract GZ 4003/2-VI/4c/2004./

7 REFERENCES

- Chan, R. C., Karl, W. C. and Lees, R. S. 2000. A new model-based technique for enhanced small-vessel measurements in x-ray cine-angiograms. *IEEE Transactions on Medical Imaging*, **19(3)**, 243-55.
- Hoffmann, K. R., Nazareth, D. P., Miskolczi, L., Gopal, A., Wang, Z., Rudin, S., and Bednarek, D. R. 2002. Vessel size measurements in angiograms: a comparison of techniques. *Medical Physics*, **29(7)**, 1622-33.
- Janssen, J. P., Koning, G., de Koning, P. J., Bosch, J. G., Tuinenburg, J. C., and Reiber, J. H. 2005. A new approach to contour detection in x-ray arteriograms: the wavecontour. *Investigative Radiology*, **40(8)**, 514-20.
- Mayr, M and Quatember, B. 2005. Segmentation of the coronary arteries in biplane angiograms based on a differential geometric approach. In F. Pistella Spitaleri and R. M., editors, *MASCOT05*, volume **10** of *IMACS Series in Computational and Applied Mathematics*, 71-80, Lecce, Italy.
- Quatember, B., Mayr, M. and Recheis, W. 2007. Image-based simulation of the three-dimensional coronary blood flow. In *MODSIM 2007 Congress*, Christchurch, New Zealand.
- Quatember, B. and Mühlthaler, H. 2003. Generation of cfd meshes from biplane angiograms: an example of image-based mesh generation and simulation. *Applied Numerical Mathematics*, **46(3-4)**, 379-97.
- Reiber, J. H., van der Zwet, P. M., Koning, G., von Land, C. D., van Meurs, B., Gerbrands, J. J., Buis, B., and van Voorthuisen, A. E. 1993. Accuracy and precision of quantitative digital coronary arteriography: observer-, short-, and medium-term variabilities. *Catheterization and Cardiovascular Diagnosis*, **28(3)**, 187-98.
- Schrijver, M. and Slump, C. 2002. Automatic segmentation of the coronary artery tree in angiographic projections. *Proceedings of BroRISC 2002*, November 28-29, 2002, Veldhoven, cNetherlands, pages 449-464.
- Silver, K. H., Buczek, J. A., Esser, P. D., and Nichols, A. B. 1987. Quantitative analysis of coronary arteriograms by microprocessor cinevideodensitometry. *Catheterization and Cardiovascular Diagnosis*, **13(5)**, 291-300.